R&D REPORT No. 74

Predicting heat and mass transfer during bread baking

1999

Campden BRI

Campden BRI

Chipping Campden Gloucestershire GL55 6LD, UK

Tel: +44 (0)1386 842000 Fax: +44 (0)1386 842100 www.campden.co.uk

R&D Report No. 74

Predicting heat and mass transfer during bread baking

JE Hall, SR Otto and P Richardson

1999

Information emanating from this company is given after the excercise of all reasonable care and skill in its compilation, preparation and issue, but is provided without liability in its application and use.

Information in this publication must not be reproduced without permission from the Director-General of Campden BRI

PREDICTING HEAT AND MASS TRANSFER DURING BREAD BAKING

J.E Hall¹, S.R. Otto² and P.S. Richardson¹

SUMMARY

Although apparently a simple food, bread is formed as a consequence of complex physical and chemical changes which occur during baking. To model part of this process, baking was viewed as a combination of heat gain via conduction and moisture loss through evaporation and diffusion. Surface heat gain has a strong dependence on oven type, which was assumed to be pure convection. Heat supply to the bread surface was modelled using a flux condition, which resulted in a surface temperature close to 160°C after a 30 minute bake, in good agreement with experimental results presented. To provide input for the model, several thermal and physical parameters were determined experimentally. Within the crumb, heat transfer was shown to be far more than could be accredited to heat conduction. To reflect all additional heat transfer mechanisms, 'effective' thermal properties were used. Predicted temperatures within the entire crumb were close to 100°C after baking, whilst the water content remained close to its initial level of around 45% of total weight. At the end of baking, the predicted moisture level in the crust was close to zero. Practical trials showed that the models were in good agreement with measured results, paving the way for these models to be used in process optimisation studies. Such studies will enable the optimisation of production throughput, product quality and heat transfer mechanisms.

¹Department of Process & Product Development, CCFRA

²School of Mathematics & Statistics, University of Birmingham



CONTENTS

Page Nu	mber
---------	------

1.	INT	RODUCTION AND BACKGROUND	1
2.	MOI	DEL DEVELOPMENT	5
	2.1	Model Equations	7
3.	NUM	MERICAL SOLUTION	9
4.	THE	RMO-PHYSICAL PARAMETER	12
	4.1	Specific Heat Capacity	12
	4.2	Thermal Conductivity	15
	4.3	Density	16
	4.4	Thermal Diffusivity	18
	4.5	Moisture Diffusivity	21
5.	RES	ULTS AND DISCUSSION	24
	5.1	One-dimensional Model Solution	24
	5.2	Validation of Predicted Moisture Level and Crust Thickness	26
	5.3	Two-dimensional Model Solution	29
6.	CON	ICLUSIONS	32
7.	ACK	NOWLEDGEMENTS	32
8.	REF	ERENCES	32
	APP	ENDIX I	34
	Mod	el Equations	



1. INTRODUCTION AND BACKGROUND

A validated model of the heat and mass transfer that takes place during bread baking is one key to being able to optimise process parameters with final product quality.

The physical and chemical changes that take place during bread baking are complex and depend on many interacting factors (Marston and Wannan, 1979). Temperature change within the dough/crumb occurs in three phases. These are an initial lag phase followed by a steep rise in temperature with an inflexion at 85°C before the temperature continues in an asymptotic approach to the boiling point of water. Once all unbound water has evaporated, the crumb is referred to as crust, with a temperature which rises approaching oven temperature. The evaporation front advances inwards towards the centre of the bread during baking and consequently the crust thickens (Zanoni and Peri, 1993).

A phenomenological model of the baking process was proposed by Zanoni and Peri (1993) and later developed into a mathematical model (Zanoni, Pierucci and Peri, 1994). An axi-symmetric model was developed in cylindrical coordinates and experimentally validated with dough baked in a cylindrical mould inside a forced convection electric oven. The dough recipe used to validate the model incorporated baking powder as a raising agent, as opposed to the type of yeasted bread dough used in the work reported here. The upper surface of the bread was heated by convection, the sides and base by combined convective and conductive heat transfer. Heat supply by radiation was minimised by cooling the oven walls with an air-space circulation system; the mould was supported by a glass holder to avoid supply by conduction.

Although the bread dough used by Zanoni and Peri (1993) and Zanoni, Pierucci and Peri (1994) was quite different to the type of bread dough focused on here, the modelling techniques employed are equally valid. The model equations describe the combination of heat transfer by conduction and moisture loss by diffusion and evaporation. The process is dependent on various thermal and physical parameters. Relationships between these and the changing temperature and moisture content are given. However, the validity of the transport equations presented by these authors is limited to cases where the heat conduction and moisture diffusion rates have no spatial

dependence. In the work outlined here, similar equations are presented in their generalised form, to allow thermo-physical parameters to vary spatially with moisture content and temperature.

Bread baking is not the only process involving heat gain and moisture loss which has been modelled mathematically. Farkas, Singh and Rumsey (1996a,b) developed and validated a model of heat and mass transfer for immersion frying. A moving boundary formulation (Landau, 1950) was used to model a dry outer crust and moist inner core, with an interface temperature of 100°C. The model and experimental data were in good agreement for temperature and moisture profiles as well as crust thickness. Chen and Moreira (1997) have also investigated this type of process, modelling the batch deep-frying of tortilla chips. In this work the authors have avoided the need to employ a moving boundary formulation by defining complex governing equations for temperature change and mass transfer which are valid in both crust and core. This type of approach is very similar to that used by Zanoni, Pierucci and Peri (1994), and has been adopted in the work reported here.

Values for several thermo-physical parameters are necessary as input for a mathematical model. Rask (1989) compiled a review of published data, presenting thermal properties of dough and other bakery products. Thermal properties of bread continuously change during baking due to increasing volume, decreasing moisture content and increasing temperature. Thermal conductivity of bread rolls decreases with time, due mainly to gas expansion (Bakshi and Yoon, 1984) and has been related to moisture content and density using regression analysis of experimental data. Well fitting regression equations have also been used to relate density to time, the limitation being that the equation generated is only valid for the situation in which the data was gathered.

Several authors have tried to use more general approaches to represent changes in the thermal properties during baking. In many cases, values of the parameters are given for water and for 'dry matter', with the corresponding value for bread calculated as a weighted average of the two according to the volume or mass fraction of water in the bread. Hallström, Skjöldebrand and Trägårdh (1988) used volume fractions to calculate an apparent conductivity for a layered material, proposing different weightings depending on whether the heat flow is perpendicular to the layers, or parallel. Upper and lower bounds for the conductivity of a completely random

heterogeneous material can be calculated: the conductivity calculated assuming parallel layers gives an upper bound whilst that calculated assuming perpendicular layers gives a lower bound. Using a value between the upper and lower bounds, Tadano (1987) estimated the conductivity of the solid part of white bread by combining the parallel and perpendicular weightings in a 'seriesparallel' (mixed) method.

To calculate the specific heat capacity (C_p) of a material, the specific heat capacities of the individual components should be weighted according to their mass fractions. Johnsson and Skjöldebrand (1984) take the specific heat of bread to be the sum of the products of mass fraction with specific heat for water and for 'dry matter'. Specific heat capacity of crust and crumb were investigated separately and a well fitting equation describing their temperature and water content dependence was obtained. For the water contents investigated, the deviation from the curve was not more that 5-10% of the actual value. Bakshi and Yoon (1984) also used this method to determine the specific heat capacity of bread rolls with the moisture content calculated from a regression relationship with time. No indication was given as to how well this relationship performed against measured data.

In the work described in the sections that follow, volume and mass fractions of air, solid and water have been used in this way to estimate the thermal properties of bread during baking. During the course of this work, however, it became apparent that this technique was not sufficiently accurate to describe the heat transfer that takes place within the bread crumb. This is because heat conduction is not the principle method of heat transfer within the crumb during baking. The temperature rise is accelerated by some other heat transfer mechanism, such as convection within the pores or via water vapour movement. Whatever the process, this additional heat transfer would be extremely complex to model, due to the varying structure of the dough. To overcome this, baking was modelled as a process of heat conduction using 'effective' thermal properties to account for the additional heat transfer.

As well as values for the thermal properties, values for parameters governing the evaporation and diffusion of moisture are required to model bread baking. To progress, it is necessary to determine the diffusion rate of water in bread crumb and crust. As an estimate for this, in the work contained in the following sections, the diffusivity of water in baked bread was taken to be

the same as that in uncooked bread dough. As moisture diffusion in both baked and un-baked bread dough is very low, this assumption should yield reasonable results. Diffusion coefficients can be calculated by fitting analytic solutions of Fick's second law (Crank, 1975) to experimental drying data. This method was successfully used by Karathanos and Kostaropoulos (1995) to determine the diffusion rate of water inside dough/raisin mixtures as part of a study on the storage stability of bakery products. Dural and Hines (1992) also used this approach to calculate the diffusivity of water in cereal fibres.

The aim of the work reported in the sections that follow was to develop a validated mathematical model of the heat and mass transfer that occurs during bread baking. Model predictions are useful for ensuring that the loaf centre temperature reaches an adequate level for structure development. These also enable investigations into the effect of oven conditions on moisture loss and temperature gain, leading to optimisation of bread baking times with the potential to improve plant performance and increase yields.

The model equations are outlined in section 2, with details of the numerical solution contained in section 3. As input to the model equations, knowledge of several thermal and physical parameters is required. These have been determined experimentally and related to moisture level, temperature and dough density; details of these parameters are contained in section 4. Model equations have been solved in both one and two dimensions, the results of which are illustrated in section 5. Model predictions are validated with the temperature and moisture level within a standard 800 g white loaf after a 30 minute baking time.

2. MODEL DEVELOPMENT

Within this section, experimental temperature profiles are first presented to provide insight into the physics involved in bread baking. Model equations which reflect this physical situation are then presented in a generalised form. The equations rely on several thermal and physical parameters which vary throughout baking, according to temperature, moisture level and volume fraction of air. The parameters are defined here but are described in more detail in section 3.

Model equations were set up under the assumption that during baking, bread dough temperature rises to 100°C, where it remains until water has evaporated, then increases asymptotically towards the oven temperature. This was verified by baking bread dough produced using a recipe representative of a standard commercially available 800 g white sliced loaf (yeast, salt, fat and ascorbic acid at 1.5%, 2%, 1% and 0.01% of flour weight respectively; variable weights of water and fungal amylase were added according to farinograph results). The dough contained in a steel tin (12.5 cm high, 12.2 cm wide, 25.0 cm deep) was proved to a height of 11 cm at 43°C, then baked with a lid on for 30 minutes at 244°C in a Bone 'Masterbaker ' direct gas-fired 12 tray reel oven.

Temperatures within the bread and the baking chamber were measured using thin-wire type-T thermocouples. One probe was positioned close to the bread tins to give an indication of how variable the oven temperature was. It can be seen in Figure 1 that the temperature outside the bread tins was indeed very variable, with a cyclic pattern induced by the movement of the oven trays. At the interface between the bread dough and the base of the tin, a temperature close to 160° C was reached after 30 minutes baking, whereas at 1 and 3 cm from the base, temperatures were close to 100° C (Figure 1).

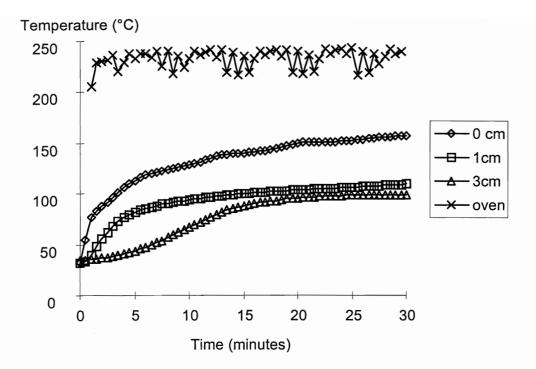


Figure 1: During a 30 minute bake, bread dough temperatures at 0, 1 and 3 cm from the base of an 800 g loaf tin, remained relatively constant at 100°C whilst unbound water evaporated. Extending the heating time would eventually allow these temperatures to approach oven temperatures.

The large amount of air entrained within bread dough is associated with low thermal conductivity, giving rise to steep temperature gradients. Within the crumb, the temperature gradients are small, even after just 30 minutes. It is unlikely that the bread dough is heating entirely by conduction; more likely is that some other heat transfer mechanism is also in force. Additional heat transfer could be due to convection within the pores, or water vapour movement. This is a complex situation to model, so for the scope of this work baking has been modelled as a heat conduction process using 'effective' thermal properties. These 'effective' thermal properties enable the model to take account of all types of heat transfer, without determining them explicitly.

2.1 Model equations

Identifying the physics involved in bread baking was a necessary step towards defining model equations. During the baking time (t), heat (T) is transferred internally by conduction,

$$\rho C_p \frac{\partial T}{\partial t} = \nabla . (k \nabla T), \tag{1}$$

at a rate controlled by the dough density (ρ) , specific heat capacity (C_p) and thermal conductivity (k). The three thermal properties (ρ, C_p, k) are liable to change with temperature and moisture content which varies spatially and temporally. During baking, the volume of the bread will also change due to gas expansion. This has been accounted for within the model equations by allowing the spatial variables to take values between zero and a function of time (see Appendix I for full details).

With an oven temperature in excess of 100°C, some point within the bread dough will eventually reach 100°C. At this point equation (1) becomes invalid as all heat transferred is used to evaporate moisture so that the temperature remains constant, that is

$$\frac{\partial T}{\partial t} = 0. (2)$$

The location of this point at 100°C defines the evaporation front. Once the local moisture has evaporated, the conduction heating resumes, until the temperature at this point eventually equals the oven temperature.

Surface heat transfer is dependent on the oven temperature (T_{amb}) , convection within the oven (h), tin thickness (δ) and tin conductivity (k_t) ,

$$k\frac{\partial T}{\partial t} = \pm \frac{\left(T - T_{amb}\right)}{\left(\frac{1}{h} + \frac{\delta}{k_{t}}\right)},\tag{3}$$

the sign being dependent on the direction of heat transfer. During bread baking the two terms on the bottom of the right hand side are comparable in size as the effects of convection and conduction are commensurate. The use of this boundary condition on all sides of the loaf assumes free movement of air all around the tin. In reality, the base of the tin is likely to be in contact with the oven tray, with heat supplied by conduction alone. Also, during the early stages of baking the top of the bread dough will not actually be in contact with the tin lid. For the scope of the work contained here, these factors have been neglected, but could be accounted for by modifications to the boundary conditions.

Local water level (W) was defined on a wet basis as kg of water per kg of dough, and can therefore take values from 0 to 1. Moisture is able to move through the bread dough during baking by diffusion,

$$\frac{\partial W}{\partial t} = \nabla . (D\nabla W) \tag{4}$$

at a rate determined by the diffusion rate, D. While the temperature is at 100° C, the latent heat of vaporisation (L) is incorporated into an additional temperature dependent term,

$$\frac{\partial W}{\partial t} = \nabla \cdot \left(D\nabla W\right) - \frac{1}{\rho L} \left(\nabla \cdot \left(k\nabla T\right)\right) \tag{5}$$

to allow evaporation to take place.

The governing equations have been briefly described in their most general form. The full set of equations used to model the baking process is contained in Appendix I. In order to make model predictions for temperature and moisture content, it was necessary to solve the governing equations either analytically or numerically. Experimentally determined parameters were also required to provide input to the model, so that meaningful results could be obtained. The sections that follow detail the solution procedure and the experimental techniques used to determine values for the thermal and physical properties. Results of the model are validated in section 5.

3. NUMERICAL SOLUTION

This section contains an explanation of the techniques used to solve the governing equations contained in Appendix I. The complexity of the equations means that an analytic solution is likely to be cumbersome and possibly unobtainable. For this reason, the model equations were solved numerically and the details of the procedure used are contained here.

To allow for volume change due to gas expansion, the model equations were defined for time dependent spatial variables. Prior to solving the equations numerically, a change of variable was performed to remove this time dependence and allow a fixed grid to be used. Full details of this procedure are contained in Appendix I. The transformed equations were then discretised using finite difference approximations and solved. To ensure that a reasonable number of grid points were placed within the crust, without requiring an uneconomic number of grid points within the crumb, an irregular grid was used (Croft and Lilley, 1977). The uneven grid spacing was defined using a symmetric geometric progression (GP), with an adjustable common ratio. In the results that follow, the ratio for the GP was set at 1.3. For integrating the model in time, an implicit method was chosen as explicit methods are only stable for very small time steps. The second-order standard implicit finite difference scheme (Sod,1985; Hill and Dewynne, 1987) is stable for all time steps; however, in more than one dimension it is computationally uneconomical. This limitation was overcome by using two half time steps to advance each full time step, with each half time step only treating terms associated with a particular co-ordinate direction implicitly. This was done using the alternating direction implicit (ADI) method (Fletcher, 1991).

The governing equations discontinuously change from (1) and (4) to (2) and (5) when the temperature reaches 100° C and back again once all the moisture has evaporated. Before the model equations could be discretised using finite-difference approximations and solved, it was necessary to employ continuous functions to smooth out these discontinuities. Using a steepness constant Δ_I , the function

$$f_1(T) = \frac{1}{2} \left(1 - \tanh \left(\frac{T - 100}{\Delta_1} \right) \right)$$

was used to switch off the heat supply by conduction at 100°C, and switch on moisture loss due to evaporation. For the value $\Delta_I = 2$ the function f_1 is plotted in Figure 2.

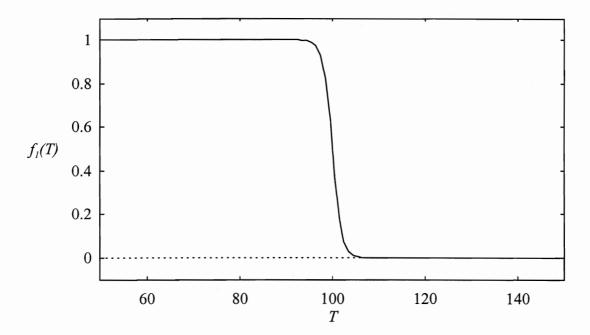


Figure 2: The function f_1 was used to switch off the heat supply by conduction at 100°C, while moisture evaporates.

The function

$$f_2(W) = \exp\left(-\frac{W^2}{\Delta_2}\right)$$

was used to switch moisture loss through evaporation off and heat supply by conduction back on once water has evaporated. Figure 3 shows the function f_2 for Δ_2 =0.01.

The functions f_1 and f_2 were used to approximate a discontinuous set of governing equations with a continuous set. The smaller the values that the constants Δ_I and Δ_2 take, the more closely the continuous equations mimic the discontinuous set. The downside to using small values for the constants Δ_I and Δ_2 is that correspondingly small time steps are necessary to provide stability. The values of Δ_I and Δ_2 found to offer the best compromise were Δ_I =10 and Δ_2 =0.01. The disparity in values for the two constants is due to the different scales defined for T and T0.1 s are required for stability.

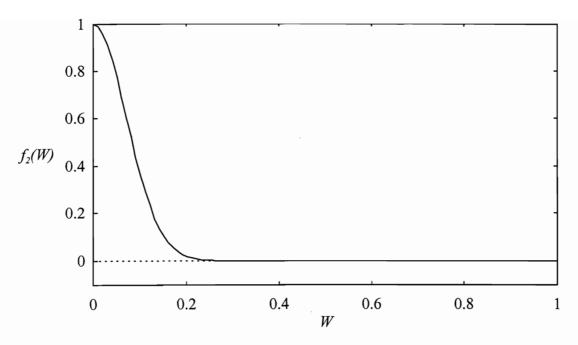


Figure 3: The function f_2 was used to switch heat conduction back on, once all local moisture had evaporated.

Once transformed into a continuous set, the model equations were solved using experimentally determined values for the parameters. A full description of the parameters and the experimental techniques used is contained in the following section. Model results are then presented in section 5 and shown to be in good agreement with experimental data.

4. THERMO-PHYSICAL PARAMETERS

Knowledge of several thermal and physical parameters was necessary so that the model equations could be solved and compared with experimentally determined temperatures and moisture levels. This section details the experimental methods used to determine specific heat capacity, thermal conductivity, density, thermal diffusivity and moisture diffusion rate. All of the properties were determined using an unyeasted dough, containing little or no air and with a known moisture content. This was done because the thermal and physical properties are known to vary during baking with temperature, moisture content and volume fraction of air. The value of each thermal property was determined for unyeasted dough, then the value for the solid part of the dough estimated by subtracting the value of the property for water, weighted with its volume or mass fraction. The way the thermal properties change during baking was then reflected in the model as the changing temperature and volume/mass fractions of air, water and dough solids were calculated.

This approach was found to work well to model the changing thermal properties within the crust. However, to model the changing thermal properties within the crumb it was found necessary to employ a different method. This is because heat transfer within the crumb involves mechanisms other than simple heat conduction. To account for all of the heat transfer mechanisms, 'effective' thermal properties were used.

4.1 Specific heat capacity

The specific heat capacity (C_p) of bread dough changes during baking according to the decreasing moisture level and increasing temperature. This was modelled by weighting the specific heat capacities of the water (C_{pw}) and the dry part of the dough (C_{pd}) according to their respective mass fractions (W and 1-W),

$$C_{p} = WC_{pw} + (1 - W)C_{pd} \tag{6}$$

(Johnsson and Skjöldebrand, 1984; Bakshi and Yoon, 1984). The specific heat capacity of water is almost constant within this temperature range and was assigned the value 4200 J.kg⁻¹.K⁻¹. The specific heat capacity of the dry part of the dough was calculated by measuring the specific heat capacity of dough with a known water content. An unyeasted dough was used under the assumption that the small amount of yeast that was missing would have little effect on the

specific heat capacity. Leaving out the yeast meant that the dough did not expand during testing, making it far easier to handle.

The specific heat capacities of unyeasted dough and bread crumb were measured using a Perkin-Elmer Pyris 1 differential scanning calorimeter (DSC, Perkin-Elmer Ltd, Beaconsfield, Bucks, UK) using the classical three curve method. As well as scanning a sample of dough, two empty pans were scanned to obtain the base-line curve and a sample of sapphire (of known specific heat capacity) was scanned to provide a reference curve. The no-sample run provides the baseline from which deflection due to heat capacities of dough and sapphire were measured. The rate of heating applied was 10°C per minute. Samples were hermetically encapsulated to prevent loss of moisture from the dough during the heating run.

Figure 4 shows the specific heat capacity of unyeasted dough increasing with temperature. The curve is irregularly shaped due to the effect of starch gelatinisation at around 60°C, but can be approximated by

$$C_p = 4200W + (1 - W)(5.96T + 1280) (7)$$

assuming a water content of 45%. Specific heat capacity measurements were also taken on bread crumb which was known to have approximately the same moisture content as the unyeasted bread dough. The specific heat capacity curves for bread dough and bread crumb were very similar, indicating that structural changes (air bubbles etc) that take place within dough during baking have little effect on specific heat capacity. This similarity between the curves for bread dough and bread crumb lends credence to the use of an equation which calculates specific heat capacity from the respective mass fractions of the components (equations (6) and (7)).

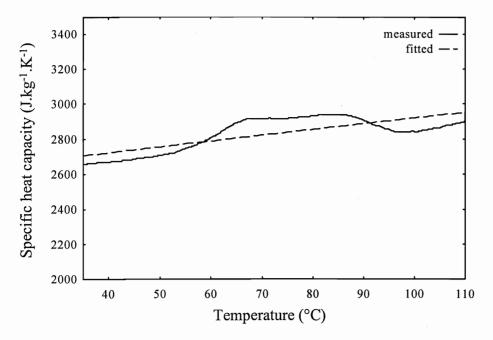


Figure 4: A straight line was fitted to experimental specific heat capacity data for input into the model.

For comparative purposes, the volumetric specific heat capacity was also measured. Volumetric specific heat capacity is defined as the product of specific heat capacity and density, and was measured using a ThermoLink (Labcell, Basingstoke, Hampshire, UK). The ThermoLink uses a heater and type E (chromel/constantan) thermocouple to find the thermal properties of the medium that the probe is inserted into. Results presented in Figure 5 are the mean and 95 % confidence intervals calculated from five replicates for a range of temperatures. Before calculating the mean and confidence interval, outlying data points were eliminated using

Dixon's test. The 95% confidence interval was then calculated as mean $\pm \frac{t(0.05, n-1)\sigma}{\sqrt{n-1}}$,

where t was obtained from a table of t-distribution values, n is the number of data points and σ is the standard deviation of the data points. At approximately 30°C the specific heat capacity of unyeasted dough was determined to be 2650 J.kg⁻¹.K⁻¹ by the DSC method, which is within the 95 % confidence interval 2753 \pm 168 J.kg.⁻¹.K⁻¹ calculated as the ratio of the volumetric specific heat capacity measured by the ThermoLink to the measured dough density of 1127.5 kg.m⁻³.

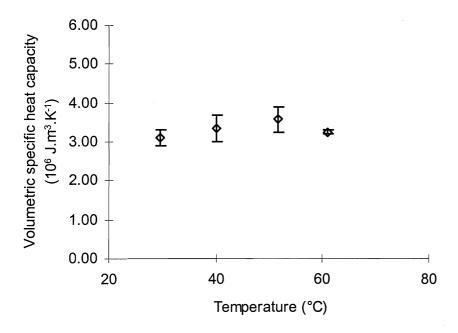


Figure 5: Volumetric specific heat capacity of unyeasted dough was found to vary with temperature.

4.2 Thermal conductivity

Thermal conductivity (k) of bread dough is dependent on the volume fractions of air (V_a) , water (V_w) and solid matter (V_s) , as well as the respective conductivities of these components (k_a, k_w, k_s) and was approximated by the linear form

$$k = V_a k_a + V_w k_w + V_s k_s \tag{8}$$

(Hallström, Skjöldebrand and Trägårdh, 1988; Tadano, 1987). To use this formula, volume fractions (V_i for i=a,w or s) were calculated from the mass fractions by multiplying by the ratio of the combined to component density $\left(\frac{\rho}{\rho_i}\right)$.

The thermal conductivity of unyeasted dough (containing little air) was measured using a ThermoLink (Figure 6). Again an unyeasted dough was used, to ensure a constant volume fraction of air whilst carrying out measurements. Assuming the unyeasted dough contained no air, the volume fractions of air, water and solid and conductivities of the dough and water were used to calculate the conductivity of the solid part of the dough. Equation (8) was then used to model the changing thermal conductivity of bread during baking.

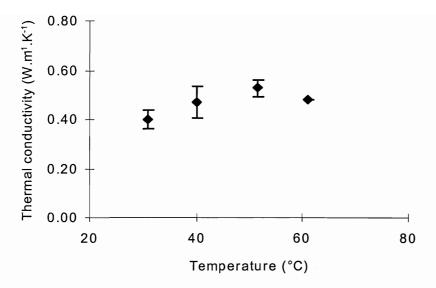


Figure 6: Thermal conductivity of unyeasted dough was found to vary with temperature.

4.3 Density

The density (ρ) of the bread dough changes during baking due to the expansion of air as well as loss of moisture. At the start of baking the dough density is approximately constant in space but after a short time the outer surface of the dough sets and the internal expansion of air leads to the formation of a dense crust surrounding the less dense crumb. Also removal of water at the evaporation front reduces bulk, causing cell collapse and a denser crust to form.

The density of yeasted and unyeasted dough was measured by placing small samples of the dough into a series of calcium chloride solutions of known densities. If the density of the sample is greater than that of the liquid then the sample immediately sinks to the bottom of the jar; if the density of the sample is less than that of the liquid then the sample floats; when dough and liquid density are equal the dough hovers below the surface, then sinks as it becomes saturated with calcium chloride. For each of the two doughs, the test was carried out twice. The density of the yeasted dough was found to be 1105 and 1115 kg.m⁻³, giving a mean value of 1110 kg.m⁻³. The density of the unyeasted dough was 1125 and 1130 kg.m⁻³, giving a mean value of 1127.5 kg.m⁻³. The difference in density between yeasted and unyeasted dough was due in part to the mass of the yeast, but may also be due to gas having already been produced in the yeasted dough.

The density of the crumb was calculated from the mass and volume of a core sample. Two replicates gave a mean density value of 196.3 kg.m⁻³. The density of the crumb was much less than that of the dough, mainly due to the high volume fraction of air. The average density of the loaf (crust and crumb) was also calculated from its mass and volume as 209.8 kg.m⁻³. Using the loaf and crumb densities, an approximate crust density was calculated as 368.3 kg.m⁻³, assuming a crust thickness of 2 mm. If instead a crust thickness of 1.5 mm had been assumed, the crust density estimate would have been 424.1 kg.m⁻³ and assuming a crust thickness of 2.5 mm the estimated density would be 334.8 kg.m⁻³. These figures are given to demonstrate how crust density has been estimated, and to give an indication of its likely bounds. As crust thicknesses and densities are liable to variation, the value of 368.3 kg.m⁻³ was taken to be representative, but this value could be adjusted at a later date if it was thought to be reducing model accuracy significantly. Varying the crust density input to the model (within this range) was found to have little impact on model results.

The difference in density between crust and crumb was modelled by the equation

$$\rho = 282.3 + 86 \tanh\left(\frac{T - 100}{\Delta_3}\right),\tag{9}$$

with Δ_3 a steepness constant which determines the density at the interface between crust and crumb. This function switches from crumb density (196.3 kg.m⁻³) to crust density (368.3 kg.m⁻³) at 100°C, the temperature at which the crust is formed. A low value of Δ_3 defines a function which switches between these two values over a small temperature range, whilst a larger value of Δ_3 provides a more gradual switch. A value of Δ_3 was chosen in part to aid the numerical solution of the model equations and in part to reflect the physical reality. This function is plotted in Figure 7 for $\Delta_3 = 2$.

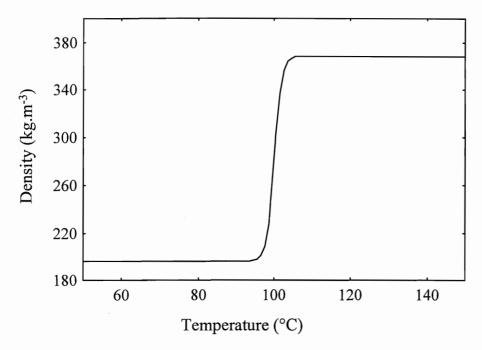


Figure 7: Density was modelled by gradually changing from crumb density to crust density at 100°C, the temperature at which crust is formed.

4.4 Thermal diffusivity

Thermal diffusivity is defined as the ratio of thermal conductivity to volumetric specific heat capacity, and is indicative of the level of heat transfer that will take place. The thermal diffusivity of unyeasted dough was measured at a range of temperatures using a ThermoLink. Results presented in Figure 8 are the mean and 95 % confidence limits calculated from four replicated thermal diffusivity measurements.

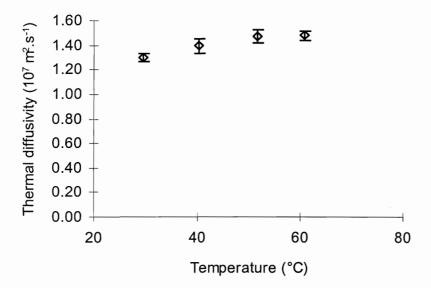


Figure 8: Thermal diffusivity of unyeasted dough was measured at a range of temperatures.

The thermal diffusivity within bread crumb was measured using the ThermoLink and found to be 2.0×10^{-7} m².s⁻¹ which is fairly low due to the high volume fraction of low conductivity air. However, experimental studies have shown that the temperature profile within bread crumb after baking is fairly uniform with a temperature close to 100° C even at the loaf centre. These high temperatures are not consistent with heat transfer by conduction alone. Heat transfer is accelerated in some way, possibly by convection within the pores, or by water vapour movement. Whatever the heat transfer mechanism, it can still be modelled as conduction, using 'effective' thermal properties to account for the additional heat transported.

The 'effective' thermal diffusivity of bread crumb was calculated from an experimental heating curve. A plot of $\log\left(\frac{100-T}{100-T_0}\right)$ against time (Figure 9) is approximately linear after an initial lag phase. For white bread a regression line with slope -0.0877 and intercept 0.5731 was fitted to the linear part of the curve with $R^2 = 0.999$. The 'heating factor' (f_h) is defined as the negative inverse of the slope of this line (Ball and Olson, 1957), in this case $f_h = 11.4$ minutes (684 s). By comparing the analytic solution for heat conduction within a brick to the equation for the fitted line, the effective thermal diffusivity (α) was calculated from the heating factor as

$$\alpha = \frac{\ln(10)}{f_h \pi^2 \left(\frac{1}{a^2} + \frac{1}{b^2} + \frac{1}{c^2}\right)}$$

using the loaf height, width and depth (a,b) and c). For a standard 800 g white loaf, the heating factor of 11.4 minutes corresponds to an 'effective' thermal diffusivity of 2.3×10^{-6} m².s⁻¹. The value of the 'effective' thermal diffusivity is roughly ten times the measured value.

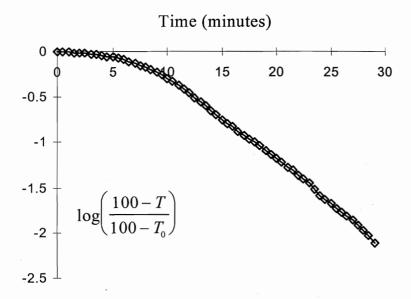


Figure 9: By plotting $\log \left(\frac{100 - T}{100 - T_0} \right)$ against time, the 'heating

factor' for white bread crumb was calculated from the slope of the linear part of the curve and then converted into 'effective' thermal diffusivity. The 'effective' thermal diffusivity was found to be approximately ten times the measured thermal diffusivity.

The same process was carried out to calculate the 'effective' thermal diffusivity of wholemeal bread (Figure 10). A line with slope -0.089 and intercept 0.8798 was fitted to the linear part of the curve with $R^2 = 0.9996$. By taking the negative inverse of the slope, the heating factor was found to be $f_h = 11.2$ minutes, corresponding to an 'effective' thermal diffusivity of 2.4×10^{-6} m².s⁻¹. The 'effective' thermal diffusivity for wholemeal bread was approximately the same as that calculated for white bread.

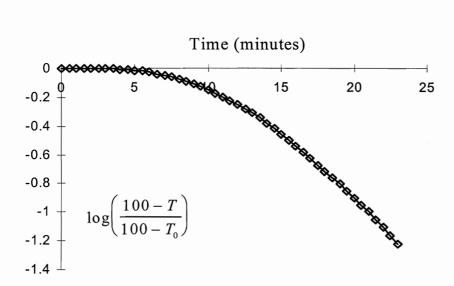


Figure 10: The 'heating factor' for brown bread crumb was calculated from the slope of the linear part of the curve and then converted into 'effective' thermal diffusivity.

The 'effective' thermal diffusivity of wholemeal bread crumb was found to be very close to the value calculated for white bread crumb.

4.5 Moisture diffusivity

As well as the thermal properties, it was necessary to determine the diffusion rate of water in bread crumb and crust. As an estimate for this, in the work contained in the following sections the diffusivity of water in baked bread has been taken to be the same as that in uncooked bread dough. As moisture diffusion in both baked and unbaked bread dough is very low this assumption should produce reasonable results.

For a simplified dough mixture, containing only flour and water, the diffusion rate was calculated using the moisture distribution method (Karathanos and Kostaropoulos, 1995). A plastic tube (12 mm diameter and 150 mm long) was half filled with a dry dough (low moisture content, W_d , typically 35%) and the other half was filled with a moist dough (high moisture content, W_w , typically 55%). The tube containing the dough was sealed at both ends with silicon and then left at an ambient temperature of 35°C for 48 hours to allow moisture to be transferred from the moist dough to the dry dough. After this time the dough was sliced using an electric slicer into 2 mm slices, the moisture content of each slice being determined gravimetrically. After several initial trials, it became apparent that even with heat treated flour and distilled water the mixture was liable to ferment within the 48 hour storage period. To stabilise the mixture,

subsequent trials were carried out using a suitable preservative (potassium sorbate at 0.3% of combined water and flour weight).

The diffusion rate (D) was then calculated by fitting the appropriate solution of Fick's second law (Crank, 1975) for composite media (Hall and Otto, 1998),

$$W = W_d + \left(\frac{W_w - W_d}{2}\right) erfc\left(\frac{x}{2\sqrt{Dt}}\right)$$
 (10)

to the moisture-distance data (W,x) for the given timescale (t=48 h). The diffusion rate D was found iteratively by using the Golden search technique (Pierre, 1969) to find the least squares solution.

Figure 11 shows the measured moisture contents within the dry portion of the dough after 48 hours storage at 35°C, with the fitted solution to Fick's second law. In this case the diffusion rate was found to be 0.7×10^{-10} m².s⁻¹, assuming the moisture content within the dough was 35.5% and in the wet dough was 54.5%. The value of the diffusion rate, D is reasonably close to the range $1.3-3.5\times 10^{-10}$ m².s⁻¹ previously reported for moisture transported from a moist raisin pulp to a dough comprising flour and distilled water (Karathanos and Kostaropoulos, 1995). These diffusion rates are fairly low, consistent with the relatively small moisture loss found within the crumb during the baking process.

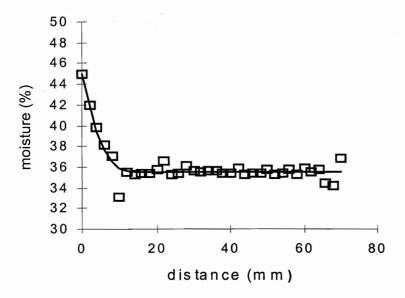


Figure 11: The diffusion rate for moisture in unyeasted dough was calculated by allowing moisture to diffuse from wet dough to dry dough, then fitting a diffusion curve(-) to the moisture-distance data (□).

The measured values for the thermal and physical parameters determined in this section have been used to predict the temperatures and moisture content within an 800 g white loaf baked for 30 minutes. Predictions were made in one and two dimensions; the results are presented and compared with experimentally determined levels in the following section.

5. RESULTS AND DISCUSSION

In this section, the values of the parameters determined in the previous section have been input into the model equations, solved in one and two dimensions. Model predictions of temperature and moisture level are presented, for an 800 g white loaf baked at 244°C for 30 minutes. In terms of temperature, moisture level and crust thickness, model results are shown to be in good agreement with those determined experimentally.

Values for the parameters not determined experimentally (detailed in section 4) were taken from published data. The heat transfer coefficient (h) was taken to be 20 W.m⁻².K⁻¹ (Croft and Lilley, 1977), the tin thickness (δ) was measured as 2 mm and assumed to have a thermal conductivity (k_t) of 45.0 W.m⁻¹.K⁻¹ (Croft and Lilley, 1977), and the value used for the latent heat of vaporisation (L) was 2.4 MJ.kg⁻¹ (Zanoni, Pierucci and Peri, 1994). The dough was assumed to be at 35°C at the start of baking, with a moisture content of 45%. The height of the bread was taken to be constant at 12.5 cm throughout baking, although in reality there was a rise from 11 cm to 12.5 cm during the early stages of baking (in the first 10 minutes). The model equations are capable of handling a variable loaf height, but in the case of a lidded loaf the increase in height was found to be small and difficult to quantify.

5.1 One-dimensional model solution

Figure 12 shows the predicted temperature profile within an 800 g white loaf. The results show good qualitative agreement with what is known to happen physically. The temperature at the edge of the bread is predicted to be just over 160°C, which is similar to the level seen experimentally in Figure 1. The temperature profile can be split into two distinct regions, one where the temperature is above 100°C and temperature gradients are high (crust) and one where temperatures are close to 100°C and gradients are small (crumb). The region of crust at both edges of the bread visually appears to be of the order of 2-5 mm. This crust thickness compares well with thicknesses found experimentally, which are presented in the following section.

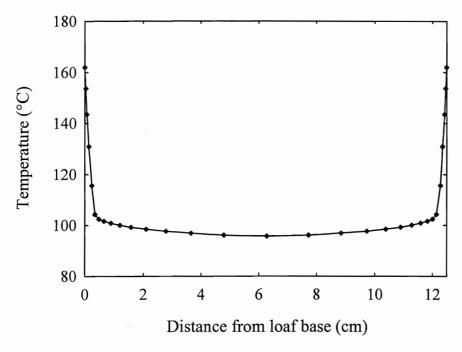


Figure 12: Model predictions show temperature within an 800 g white loaf after a 30 minute bake.

To give an indication of how well model results compare with reality, Figure 13 shows a comparison of experimentally and theoretically determined temperature profiles 3 cm into bread dough during baking. The experimental curves show considerable variation as it was very difficult to precisely position the temperature probes. The predicted temperature curve is well within the range found experimentally.

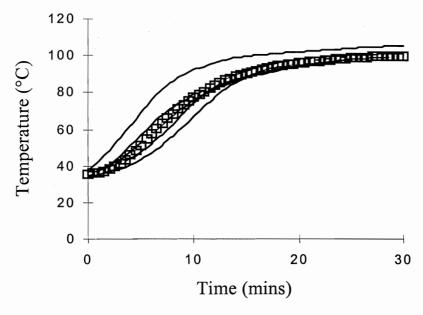


Figure 13: Comparison of measured temperatures within an 800 g white loaf (-) and model predictions (\square) shows good agreement.

Figure 14 shows the predicted moisture levels obtained alongside the temperature levels given in Figure 12. Low moisture levels are apparent within the crust, the level within the crumb has remained at its initial level and there is a steep gradient between the two regions. As with the temperature profile given in Figure 12, the crust thickness appears to be around 2-5 mm.

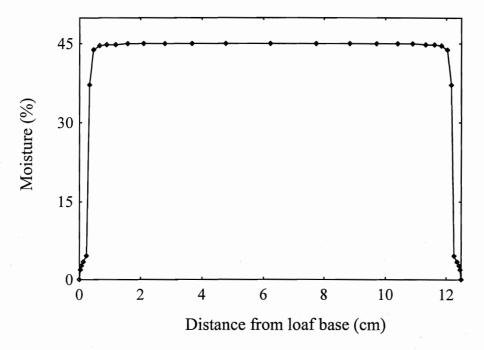


Figure 14: Model predictions of moisture content inside an 800 g white loaf after a 30 minute bake reveal little moisture loss within the crumb.

5.2 Validation of predicted moisture level and crust thickness

To determine the moisture level within the base crust, a slice was taken from the centre of the loaf, then a section of crust, away from the sides, was removed (Figure 15). A section above this, representing the outer crumb, was also removed. Samples were also taken in this way to determine the moisture level of the top and side crusts/outer crumbs. Finally a sample was taken from the centre of the slice to determine the inner crumb moisture level.

Samples were taken from loaves baked for 10, 15, 20, 25 and 30 minutes, to determine how moisture content is affected by the baking process. As the bread tins used were straps of three tins (ie three tins joined together), three loaves were baked at a time and these were numbered

1,2 and 3 from right to left. After each bake all the samples outlined above were taken from one loaf before moving onto the second and third. Three replicate bakes were carried out for each of the six cooking times (fifty four loaves in all) with samples taken using a different loaf ordering (123,231,312) for each replicate. In this way any variation in measurements caused by the loaf order could be identified and eliminated.

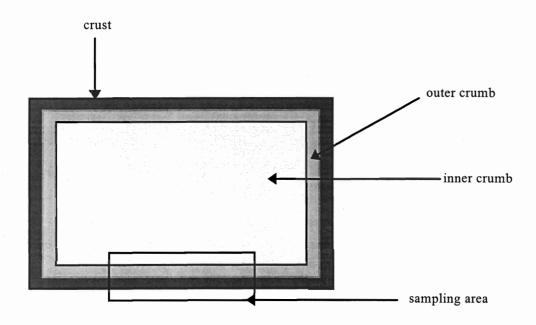


Figure 15: The moisture content of the crust and outer crumb of a slice of bread, taken from the centre of a loaf, were determined

Figure 16 is a plot of crust thickness against time for the top, base and side crusts. Each point is the mean of 9 (for top and base) or 18 (for the side) measurements. In all positions, the crust thickness with time from no crust initially to 1.5-2.5 mm after 30 minutes, indicating that model crust thicknesses seen in Figures 12 and 14 are reasonable. The crust thickness appears to rise in a linear fashion over the 30 minutes. The base crust appears to be the thickest early on in the bake. This is likely to be because the base of the tin is in direct contact with the hot oven tray. The top crust thickness more slowly, as in the early stages of baking there will be a small air gap between the bread dough and the tin lid. At the end of baking, the side crust appears to be the thinnest. This is not surprising, as the value is averaged over both sides of the tin (left and right), one or both of which will be very close to its neighbouring tin's side. This means that air movement is likely to have been restricted, and consequently heat transfer.

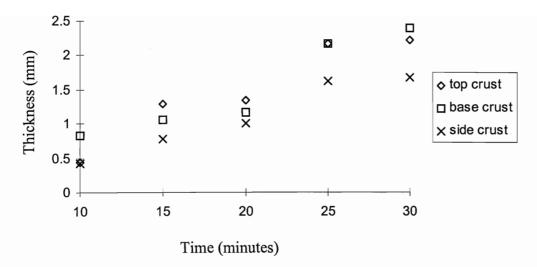


Figure 16: Top, base and side crust thicknesses were measured at different times during a 30 minute bake.

Figure 17 shows the moisture levels at various positions within the bread. Moisture levels were determined by oven drying small samples in the region of interest. The points clustered at the top of the graph are moisture levels in the inner and outer crumb regions. The graph shows that moisture levels remain fairly constant during baking, everywhere except within the crust. The slight variation between the high levels is likely to be due to sample to sample variation rather than differing levels of moisture loss. Within the top, base and side crust a significant amount of moisture was lost over the 30 minute baking time. Each point is the mean of 9 or 18 replicates and some of the variation in moisture level will be due to sample to sample variation in initial moisture content. At the end of baking the moisture levels within the crust are quite low, although not equal to zero. As the difference between crust and crumb was determined visually, it is likely that each crust sample also contained a small amount of outer crumb. Assuming this to be the case, the resulting moisture levels may be artificially high. The moisture levels for each time are very similar to those given by Zanoni and Peri (1993).

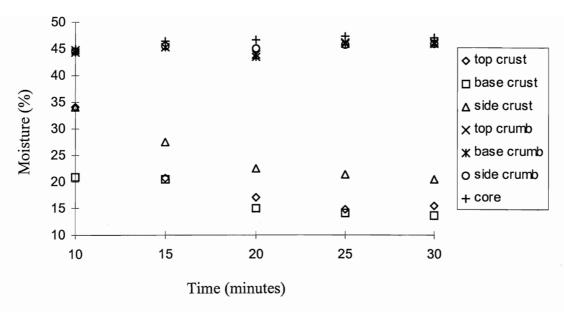


Figure 17: During baking, moisture levels within the inner (core) and outer (side, top and base) crumb were found to change very little.

5.3 Two-dimensional model solution

The model equations have also been solved in two dimensions. Figure 18 shows the predicted temperature profile along the width and height of an 800 g white loaf. As in one dimension the temperatures within the crumb are all fairly close to 100°C, whilst gradients are steep within the crust. The temperature at the edge of the bread (away from the corners) is again just above 160°C. At the corners of the bread/tin (where two sides meet) heat is supplied from two directions and subsequently much higher temperatures are predicted. In 3D, the 3D corners are likely to show even higher levels as heat is supplied from 3 directions.

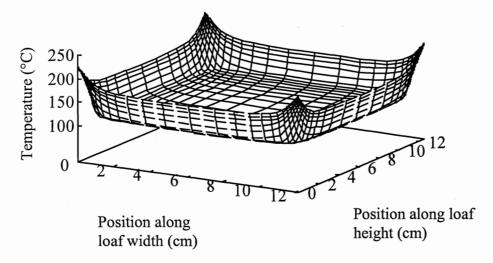


Figure 18: Where two sides of the tin meet, model predictions show that bread temperatures are high as heat is supplied from two directions.

Figure 19 shows the predicted moisture levels within an 800 g white loaf after baking. These results were found simultaneously with the temperatures shown in Figure 18. As in one dimension, it can be seen that the moisture level within the crumb has remained at its initial level (45%), with a low level inside the crumb and a steep gradient between the two regions. In addition to the features apparent in the one-dimensional model solution, the two-dimensional solution shows that slightly more moisture is lost at the bread/tin corners due to the higher temperatures seen in Figure 18.

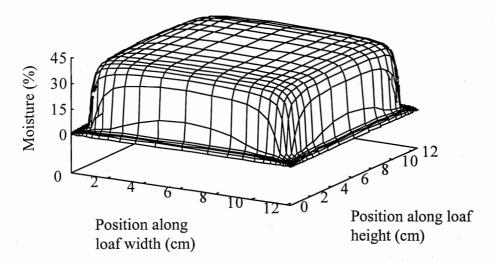


Figure 19: Model predictions show that moisture loss is greater where two sides of the tin meet, as predicted temperatures are higher here.

In a loaf of bread, there is visually very little difference between two slices taken from any position away from the end crusts. This suggests that most of the heat transfer/moisture loss can be accounted for by a two-dimensional model. Solving the model equations in two dimensions gives an indication of whether it is necessary to also solve the equations in three dimensions. Figure 20 shows two-dimensional model predictions for temperature against loaf height and depth. There is very little temperature variation along the depth of the loaf, except close to the end crusts. This suggests that a three-dimensional model would not provide any further information (except about 3D corners), merely increasing the computational costs involved. As further verification, Figure 21 shows the corresponding moisture profile, again with little variation along the depth of the loaf.

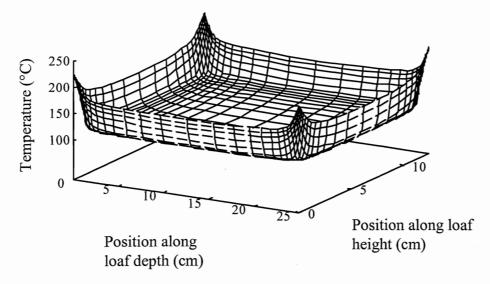


Figure 20: The two-dimensional model can be used to look at a 2D slice along the depth of a loaf as well as a 2D slice along the width of a loaf. Very little temperature difference is predicted along the depth of the loaf except close to the end crusts.

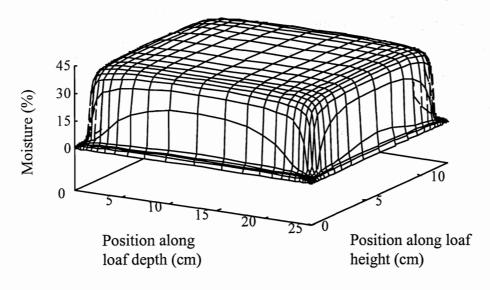


Figure 21: Model predictions show that moisture variation along the depth of a loaf is minimal, with the majority of moisture lost from the crust.

6. CONCLUSIONS

Baking bread involves heating the bread dough above the atmospheric boiling point of water. For this reason, moisture loss and temperature gain must be considered simultaneously when attempting to develop a mathematical model. In the work presented here, equations which couple heat and mass transfer have been used to predict temperature and moisture change within bread during baking. The heat transfer involved in bread baking is a combination of heat conduction and other heat transfer mechanisms. Rather than try to explicitly define all types of heat transfer, the equations were set up assuming heat conduction alone. Any additional heat transfer taking place was accounted for by using 'effective' thermal properties.

A flux condition was used to simulate heat transfer to the bread surface, and gave a surface temperature close to 160°C, in good agreement with that found experimentally. Predicted temperature and moisture levels show a split between crust and crumb, with an evaporation front between them. Within the crumb, model temperatures were below 100°C and moisture remained at its initial level. The crust was shown to be fairly dry with a temperature in the range 100-160°C.

The models and practical measurements were in good agreement and, as such, the models offer the potential to carry out product or process optimisations to improve the quality of product and/or the efficiency of the manufacturing process through an improved understanding of the heat and mass transfer operations governing bread baking.

7. ACKNOWLEDGEMENTS

Much of the programming was carried out by Victoria Bravington (School of Mathematics, University of Wales, Cardiff), during her industrial placement year, for which the authors are extremely grateful. The authors would also like to thank Andrew Keene (Department of Baking and Cereal Processing, CCFRA) for all his help with the experimental validation.

8. REFERENCES

Bakshi, A.S. and Yoon, J. (1984). Thermo-physical properties of bread rolls during baking. Lebensmittel-Wissenschaft und Technologie, 17:90-93.

Ball, C. O. and Olson, F. C. W. (1957). Sterilization in food technology. Theory, practice and calculation. McGraw-Hill, New York, USA.

Chen, Y. and Moreira, R.G. (1997). Modelling of a batch deep-fat frying process for tortilla chips. Transactions of the Institute of Chemical Engineers, Part C, 75:181-190.

Crank, J. (1975). The mathematics of diffusion. Published by Oxford University Press, Oxford, UK.

Croft, D.R. and Lilley, G. (1977). Heat transfer calculations using finite difference equations. Applied Science Publishers, London.

Dural, N.H. and Hines, A.L. (1992). Diffusion of water in cereal-bread type food fibers. Journal of Process Engineering, 15:115-130.

Farkas, B.E., Singh, R.P. and Rumsey, T.R. (1996a). Modeling heat and mass transfer in immersion frying. I, model development. Journal of Food Engineering, 29:211-226.

Farkas, B.E., Singh, R.P. and Rumsey, T.R. (1996b). Modeling heat and mass transfer in immersion frying. II, model solution and verification. Journal of Food Engineering, 29:227-248.

Fletcher, C.A.J. (1991). Computational techniques for fluid dynamics. Vol. 1. Springer Verlag, Heidelberg, pp 252-255.

Hall, J.E., Bravington, V. and Otto, S.R. (1998). Simulation of the transition from dough to bread. ACoFoP IV Symposium proceedings, 503-509.

Hall, J.E and Otto, S.R (1998). A study of the diffusion of oxygen in composite media. Submitted to Journal of the Australian Mathematical Society, Series B (Applied Mathematics).

Hallström, B., Skjöldebrand, C. and Trägårdh, C. (1988). Heat transfer and food products. Elsevier Applied Science, London.

Hill, J.M. and Dewynne. (1987). Heat conduction. Blackwell Scientific Publications.

Johnsson, C. and Skjöldebrand, C. (1984). Thermal properties of bread during baking. In: Engineering of food, Vol. 1, ed. B. M. McKenna. Elsevier Applied Science, London, pp 333-341.

Karathanos, V.T. and Kostaropoulos, A.E. (1995). Diffusion and equilibrium of water in dough/raisin mixtures. Journal of Food Engineering, 25:113-121.

Landau, H.G. (1950). Heat conduction in a melting solid. Quarterly of Applied Mathematics, 8(1):81-94.

Marston, P.E. and Wannan, T.L. (1976). Bread baking: the transformation from dough to bread. The Bakers Digest, August:24-49.

Pierre, D.A. (1969). Optimization theory with applications. Wiley, New York...

Rask, C. (1989). Thermal properties of dough and bakery products: a review of published data. Journal of Food Engineering, 9:167-192.

Sod, G.A. (1985). Numerical methods in fluid dynamics. Cambridge University Press.

Tadano, T. (1987). Thermal conductivity of white bread. Bulletin of the College of Agricultural and Veterinary Medicine, 44: 18-22.

Zanoni, B. and Peri, C. (1993). A study of the bread baking process - I. phenomenological model. Journal of Food Engineering, 19:389-398.

Zanoni, B., Pierucci, S. and Peri, C. (1994). Study of the bread baking process - II. Mathematical modelling. Journal of Food Engineering, 19:321-336

APPENDIX I - Model equations

Nomenclature

specific heat capacity (J.kg⁻¹.K⁻¹) moisture diffusion rate (m².s⁻¹) C_p

oven to tin heat transfer coefficient (W.m⁻².K⁻¹) h

k

thermal conductivity (W.m⁻¹.K⁻¹) latent heat of vaporisation (J.kg⁻¹) L

Ttemperature (K)

time (s)

spatial variable (m) \boldsymbol{x}

moisture content (wet basis, kg.kg⁻¹) W

thermal diffusivity (m².s⁻¹) α

bread tin wall thickness (m) δ

water content at which evaporation stops (kg.kg⁻¹)

density (kg.m⁻³)

Subscripts

oven value amb

boiling point value bp

initial value

Superscript:

non-dimensional parameter

The general form of the equations used to model heat gain and moisture loss was

$$\rho C_{p} \frac{\partial T}{\partial t} = p_{1}(W, T) [\nabla \cdot (k \nabla T)]$$

$$\frac{\partial W}{\partial t} = \nabla \cdot (D \nabla W) - p_{2}(W, T) \left[\frac{1}{\rho L} (\nabla \cdot (k \nabla T)) \right]$$
when $t > 0$

with $T=T_0$ and $W=W_0$ initially. The functions p_1 and p_2 were used to switch heat transfer and moisture evaporation on/off and are defined in dimensionless form at the end of this section.

In one dimension the associated boundary conditions were

$$k \frac{\partial T}{\partial t} = \frac{\left(T - T_{amb}\right)}{\left(\frac{1}{h} + \frac{\delta}{k_{t}}\right)}$$
 and $W = \varepsilon$, where $x = 0$

and

$$k \frac{\partial T}{\partial t} = -\frac{\left(T - T_{amb}\right)}{\left(\frac{1}{h} + \frac{\delta}{k_{t}}\right)}$$
 and $W = \varepsilon$, where $x = x_{0}g(t)$

The model equations were non-dimensionalised using

$$T^{+} = \frac{T - T_{0}}{T - T_{amb}}, \ W^{+} = \frac{W}{W_{0}}, \ x^{+} = \frac{x}{x_{0}g(t)}, \ t^{+} = \frac{\alpha_{0}t}{x_{0}^{2}}$$

which removed the time dependence from the spatial variable and transformed the governing equations into

$$\alpha_0 \rho C_p \frac{\partial T^+}{\partial t^+} = \left(f_1^+ \left(W^+, T^+ \right) \frac{1}{g^2} \frac{\partial k}{\partial x^+} + \alpha_0 \rho C_p x^+ \frac{g'}{g} \right) \frac{\partial T^+}{\partial x^+} + f_1^+ \left(W^+, T^+ \right) \frac{k}{g^2} \frac{\partial^2 T^+}{\partial x^{+2}}$$

$$\partial W^+ = \left(1 - \partial D - g' \right) \partial W^+ - D \partial^2 W^+$$

$$\alpha_{0} \frac{\partial W^{+}}{\partial t^{+}} = \left(\frac{1}{g^{2}} \frac{\partial D}{\partial x^{+}} + \alpha_{0} x^{+} \frac{g^{\prime}}{g}\right) \frac{\partial W^{+}}{\partial x^{+}} + \frac{D}{g^{2}} \frac{\partial^{2} W^{+}}{\partial x^{+^{2}}}$$

$$- f_{2}^{+} \left(W^{+}, T^{+}\right) \frac{\left(T_{amb} - T_{0}\right)}{\rho L g^{2} W_{0}} \frac{\partial k}{\partial x^{+}} \frac{\partial T^{+}}{\partial x^{+}} - f_{2}^{+} \left(W^{+}, T^{+}\right) \frac{\left(T_{amb} - T_{0}\right) k}{\rho L g^{2} W_{0}} \frac{\partial^{2} T^{+}}{\partial x^{+^{2}}}$$

for $t^+>0$.

In non-dimensional form the switch functions $(p_1 \text{ and } p_2)$ were

$$p_{2}^{+} = 0.5 * \left(1 - \exp\left(-\frac{\left(W^{+} - \varepsilon\right)^{2}}{\Delta} \right) \right) \left(1 + \tanh\left(\frac{T^{+} - T_{bp}^{+}}{\Delta}\right) \right) \text{ and } p_{1}^{+} = 1 - p_{2}^{+}$$